Biochimica et Biophysica Acta 1818 (2012) 2868–2875

Contents lists available at SciVerse ScienceDirect

Biochimica et Biophysica Acta

journal homepage: www.elsevier.com/locate/bbamem

# Modulation of P2X3 receptors by spider toxins ☆

Natalia V. Kabanova [a], Alexander A. Vassilevski [b], Olga A. Rogachevskaja [a], Marina F. Bystrova [a], Yuliya V. Korolkova [b], Kirill A. Pluzhnikov [b], Roman A. Romanov [a], Eugene V. Grishin [b], Stanislav S. Kolesnikov [a,*]

[a] Institute of Cell Biophysics, Russian Academy of Sciences, Pushchino, Moscow Region 142290, Russia
[b] Shemyakin-Ovchinnikov Institute of Bioorganic Chemistry, Russian Academy of Sciences, Moscow 117997, Russia

ARTICLE INFO

*Article history:*
Received 14 May 2012
Received in revised form 18 July 2012
Accepted 20 July 2012
Available online 25 July 2012

*Keywords:*
P2X3 receptors
High-affinity desentisitization
Purotoxin
*Geolycosa* sp. spider venom

ABSTRACT

Recently, the novel peptide named purotoxin-1 (PT1) has been identified in the venom of the spider *Geolycosa* sp. and shown to exert marked modulatory effects on P2X3 receptors in rat sensory neurons. Here we studied another polypeptide from the same spider venom, purotoxin-2 (PT2), and demonstrated that it also affected activity of mammalian P2X3 receptors. The murine and human P2X3 receptors were heterologously expressed in cells of the CHO line, and nucleotide-gated currents were stimulated by CTP and ATP, respectively. Both PT1 and PT2 negligibly affected P2X3-mediated currents elicited by brief pulses of the particular nucleotide. When subthreshold CTP or ATP was added to the bath to exert the high-affinity desensitization of P2X3 receptors, both spider toxins strongly enhanced the desensitizing action of the ambient nucleotides. At the concentration of 50 nM, PT1 and PT2 elicited 3–4-fold decrease in the $IC_{50}$ dose of ambient CTP or ATP. In contrast, 100 nM PT1 and PT2 negligibly affected nucleotide-gated currents mediated by mP2X2 receptors or mP2X2/mP2X3 heteromers. Altogether, our data point out that the PT1 and PT2 toxins specifically target the fast-desensitizing P2X3 receptor, thus representing a unique tool to manipulate its activity.



## 1. Introduction

Extracellular ATP is a signaling molecule that mediates diverse cellular functions *via* multiple metabotropic P2Y and ionotropic P2X purinoreceptors [1–3]. P2X receptors are homo- or heterotrimers formed by P2X1–P2X7 subunits (in humans) that function as ATP-gated cation channels [4,5]. Although most P2X subunits are widely distributed among cell types of nearly every origin, expression of the P2X3 subunit is rather specific. Reportedly, P2X3 mRNA and/or protein locate largely in small-diameter sensory neurons, some epithelial cells, carotid body afferent neurons, enteric neurons, and taste buds [6–12]. The highly selective distribution of P2X3 and P2X2/3 receptors within the nociceptive system, including C-fiber sensory neurons detecting noxious stimuli in damaged or sensitized tissues, suggests P2X3 to be involved in pain sensation. This inference is strongly supported by studies of animals devoid of P2X3. Particularly, the genetic ablation of the *p2x3* gene in mice resulted in a markedly attenuated nocifensive phenotype, including a decreased sensitivity to thermal stimuli and injection of carrageenan or formalin [13]. Mice devoid of P2X3 or P2X2/3 receptors exhibited sensory deficit, including urinary and intestinal hyporeflexia and diminished taste responses, pointing out the key role for the P2X3 receptor in physiology of visceral organs and the peripheral taste system [13–17]. It thus appears that the P2X3 subunit is involved in sensitization of somatic and visceral afferent circuits of many types. Accordingly, P2X3-based ATP-gated channels are of significant therapeutic interest as a likely target for the treatment of certain types of pain and disorders of the visceral sensory function [18].

As showed in the recent report [19], a peptide isolated from the venom of the spider *Geolycosa* sp. exerted marked and specific inhibition of P2X3 receptors operating in sensory neurons from the rat dorsal root ganglion. When tested in animal models of inflammatory pain, this novel peptide named purotoxin-1 (PT1) manifested marked antinociceptive action [19]. Here we studied effects of PT1 and another polypeptide named purotoxin-2 (PT2) from the same spider venom on ATP-gated currents mediated by murine and human P2X3 receptors. Those were heterologously expressed in CHO cells. We found that both molecules, quite dissimilar in terms of primary structure, markedly enhanced the high-affinity desensitization of P2X3 receptors, thereby presenting a unique tool for manipulating activity of this purinoreceptor.

## 2. Methods

### 2.1. Chromatography

Our generally applied scheme of spider venom separation was reported earlier [20]. Crude venom of the spider *Geolycosa* sp. (spp.

☆ The protein sequence data reported in this paper will appear in the UniProt Knowledgebase under the accession number B3EWH0.

* Corresponding author at: 3 Institutional Str., Institute of Cell Biophysics, Russian Academy of Sciences, Pushchino, Moscow Region 142290, Russia. Tel.: +7 4967 739121; fax: +7 4967 330509.
*E-mail address:* staskolesnikov@yahoo.com (S.S. Kolesnikov).

0005-2736/$ – see front matter © 2012 Elsevier B.V. All rights reserved.
http://dx.doi.org/10.1016/j.bbamem.2012.07.016

code — A267TDLS2-KZARNA) was obtained from Fauna Laboratories (Republic of Kazakhstan). The separation of the venom was carried out as described [19]. The pure polypeptide toxin named purotoxin-2 (PT2) was isolated using a combination of size-exclusion and reverse-phase high performance liquid chromatography (RP-HPLC) with a TSK 2000SW column (Toyo Soda Manufacturing). The fraction I was further separated by RP-HPLC on a Vydac 218TP54 $C_{18}$ column (Separations Group).

### 2.2. Mass spectrometry (MS) and UV absorbance spectroscopy

Peptides were analyzed by MALDI MS and MS/MS as described [19,20]. An ultraflex TOF–TOF (Bruker Daltonik) spectrometer was used.

Absorption spectra were recorded on a U-3210 spectrophotometer (Hitachi, Tokyo, Japan). Polypeptide concentrations were determined using molar extinction coefficients at 280 nm calculated with the GPMAW program (Lighthouse data, http://www.gpmaw.com).

### 2.3. Protein chemistry

Our detailed protocols were published elsewhere [20]. Purified PT2 was reduced with dithiothreitol and alkylated with 4-vinylpyridine. N-terminal sequencing was carried out by automated stepwise Edman degradation using a Procise Model 492 protein sequencer (Applied Biosystems) according to the manufacturer's protocol.

0.5 nmol of S-pyridylethylated PT2 was dissolved in 40 μl of 80% TFA, and 1 μl of 5 M CNBr was added. The mixture was incubated overnight in the dark. Reaction products were separated by RP-HPLC on a Luna $C_{18}$ column (1×150 mm, 100 Å, 3 μm; Phenomenex). The C-terminal fragment was further redissolved in 40 μl of 100 mM Tris–HCl, pH 8.5. Hydrolysis by endoproteinase Asp-N (Sigma-Aldrich; enzyme–protein ratio of 1/25) was performed at 37 °C for 4 h. The peptide fragments were separated by RP-HPLC on the same Luna $C_{18}$ column and analyzed by MS/MS.

### 2.4. Recombinant polypeptide production

All steps were performed as described earlier for PT1 [19]. cDNA encoding recombinant PT2 (rPT2) was constructed from synthetic oligonucleotides (Table 1) using PCR. The fragment was cloned at KpnI and BamH1 restriction sites into the expression vector pET-32b (Novagen), which was used to transform *Escherichia coli* Origami B cells for protein production. rPT2 was produced as a fusion protein with thioredoxin, which was purified on a TALON Superflow Metal Affinity Resin (Clontech) according to the protocol supplied by the manufacturer. The purity of the hybrid protein was checked by sodium dodecyl sulfate polyacrylamide gel electrophoresis (SDS-PAGE). The hybrid protein was cleaved by human enterokinase catalytic subunit [21]; 1 unit per 1 mg of fusion protein, 4 h at 37 °C), and rPT2 was separated by means of RP-HPLC on a Jupiter $C_4$ semi-preparative column (250×10 mm, 300 Å, 10 μm; Phenomenex). The purity of rPT2 was checked by MALDI MS as well as by N-terminal sequencing and RP-HPLC on a Vydac 218TP54 $C_{18}$ column.

**Table 1**
Oligonucleotides used to construct the rPT2-encoding cDNA.

| Primer name | Sequence | Length |
|---|---|---|
| F | CGGGTACCGACGACGACGACAAGGCGAAAGCGTGCACGCCG | 41 |
| 1f | GCGAAAGCGTGCACGCCGCTGCTGCATGATTGTTCTCATGATCGCCACT | 49 |
| 2f | CCTGTTGTCGCGGCGATATGTTCAAGTATGTGTGCGACTGCTTCTACCC | 49 |
| 3f | GGAAGGCGAAGATAAGACGGAAGTGTGCTCTTGCCAGCAGCCGAAATCG | 49 |
| 4f | CACAAGATCGCGGAGAAGATCATCGACAAAGCGAAGACGACCCTGGGC | 48 |
| 1/2r | TATCGCCGCGACAACAGGAGTGGCGATCATGAGAAC | 36 |
| 2/3r | GTCTTATCTTCGCCTTCCGGGTAGAAGCAGTCGCAC | 36 |
| 3/4r | CTTCTCCGCGATCTTGTGCGATTTCGGCTGCTGGCA | 36 |
| R | CGGGATCCTTAGCCCAGGGTCGTCTTCGC | 29 |

### 2.5. P2X cloning

Full-length cDNA encoding the mouse P2X2 receptor (1509-bp) was isolated from testis by RT-PCR with the primers 5′-TCTTGTG GACCGAGCTCCTTG-3′ and 5′-AGGTCTGTAGCTTAGTGAGGATG-3′ and was cloned into *Sma*I site of pIRES2-EGFP plasmid (Clontech). Mouse P2X3 cDNA (1398-bp) was isolated from testis by RT-PCR with the primers 5′-CTGTGAGCACTTTCTCAGTATG-3′ and 5′-ATTCAGGTCTTAGC GGGAAGC-3′, TA-cloned into pGEM-T Easy plasmid (Promega), and subcloned into *Eco*RI site of pIRES2-EGFP plasmid. Platinum Pfx DNA polymerase (Invitrogen) was used for amplification. The human P2X3 cDNA (EX-U0084-B02 clone) provided by GeneCopoeia was subcloned into a pIRES2-EGFP vector by the authors.

### 2.6. Cell culture and transient transfection

Cells of the CHO line were routinely cultured in the F-12 Nutrient Mixture (F-12) (Gibco) containing 10% fetal bovine serum (HyClone), glutamine (1%) and the antibiotic gentamicin (100 μg/ml) (Invitrogen). Cells were grown in 12-well culture plates in a humidified atmosphere (5% $CO_2$/95% $O_2$) at 37 °C. The day before transfection, cells were transferred to 12-well culture plates at the density of $0.75–1\times10^5$ cells in 1 ml of F-12 per well. The recombinant plasmid pIRES2-EGFP/P2X3 or pIRES2-EGFP/P2X2 was transiently transfected into CHO cells by replacing the growth medium in each well with the transfection mixture usually containing 1 μg of DNA and 3 μl of Unifectin-56 (Unifect Group) in 1 ml of serum-free F-12. For co-transfection, pIRES2-EGFP/P2X3 and pIRES2-EGFP/P2X2 were taken at the ratio of 2:1. After 3 h of incubation, the transfection mixture was replaced with the normal culture medium. Cells were assayed within 24–72 h after transfection.

### 2.7. Electrophysiology

The whole-cell patch clamp approach was basically used. Ion currents were recorded and filtered at 1 kHz using an Axopatch 200A amplifier, a DigiData 1322A interface, and the pClamp8 software (Axon Instruments). Recording pipettes had a resistance of 3–5 MΩ when filled with intracellular solution containing (in mM): 140 CsCl, 1 MgATP, 10 BAPTA, and 10 HEPES-CsOH (pH 7.2). This dialyzing solution was chosen to inhibit interfering endogenous $K^+$ channels and $Ca^{2+}$-dependent channels. Cells were held at decreased potentials, typically at −30 mV, improving stability of cellular preparations. To minimize variability of cellular responses to nucleotides during 40–60 min recordings, the series resistance and cell capacitance were checked and compensated, if necessary, prior every ATP/CTP application. The basic bath solution included (in mM): 140 NaCl, 5 KCl, 1 $MgCl_2$, 1 $CaCl_2$, and 10 HEPES-NaOH (pH 7.4). External solutions were delivered by a gravity-driven perfusion system that allowed for a local exchange of the solution around the CHO cell for 200 ms and provided whole chamber perfusion at the rate of ~0.1 ml/s [22]. Experiments were carried out at room temperature of 22–25 °C.

## 3. Results

### 3.1. Purotoxin-2 (PT2) isolation and sequencing

The venom of the wolf spider *Geolycosa* sp. was investigated by us earlier and found to contain components that target mammalian neuroreceptors. In particular, ω-Lsp-IA modulating P-type calcium channels [23] and purotoxin-1 (PT1) affecting P2X3 purinergic receptors [19] were isolated and characterized in detail. Here we describe yet another active polypeptide from the same venom. Similar to PT1, it modulates P2X3 receptors and is therefore termed purotoxin-2 (PT2).

PT2 was isolated from the crude venom using a conventional procedure (Suppl. Fig. 1). The peptide-containing fraction obtained from size-exclusion chromatography was further subjected to RP-HPLC, and PT2

was acquired with >95% purity, as assessed by analytical HPLC. Its molecular mass was determined by MALDI MS and equaled to 7255.5 Da.

The complete amino acid sequence of PT2 was established by a combination of Edman degradation and selective proteolysis (Fig. 1A). The sequence was additionally verified by endoproteinase Asp-N cleavage and MS/MS analysis of the fragments. PT2 consists of 64 amino acid residues and features C-terminal amidation. This modification was assigned based on 1 Da difference between calculated and measured molecular masses of the full toxin (7256.3 Da and 7255.5 Da, respectively) and its C-terminal fragments. Eight cysteine residues most likely form 4 disulfide bonds, given that non-reduced PT2 is not prone to modification by 4-vinylpyridine, indicating the absence of free thiol groups. The polypeptide contains the principal structural motif (PSM) and extra structural motif (ESM) and therefore belongs to the class 2 of spider toxins [24]. Both motifs probably contribute to the inhibitor cystine knot (ICK) fold, which is typical for spider toxins [25,26].

### 3.2. Activity of P2X3 receptors in a heterologous system

To carry out a comparative study of PT1 and PT2 effects on mouse (mP2X3) and human (hP2X3) P2X3 isoforms under identical conditions, we used a heterologous system, that is, cultured CHO cells transiently transfected with pIRES2-EGFP/P2X3 plasmid. Cells expressing P2X3 at a sufficiently high level were identified by marked GFP fluorescence. For conclusive analysis, we accepted only recordings with no profound rundown (<20%) of P2X3 currents within 40–60 min, provided that PT1/PT2 modulated those reversibly. Important for protocols used here is the agonist-dependence of recovery of P2X3 receptors from desensitization [27]. For example, recovery of ATP-gated currents is nearly 10-fold slower than that of CTP-responses. With 30 μM ATP as agonist, the characteristic time of recovery has been estimated to be ~220 s and ~150 s for rat P2X3 and hP2X3, respectively [27,28]. To obtain a sufficient number of more or less reproducible nucleotide responses, mP2X3-positive cells were stimulated mainly by CTP. In experiments with hP2X3, ATP-gated currents exhibited a sufficiently short refractory period, so that this natural P2X agonist was largely used to examine effects of the spider toxins on the hP2X3 isoform.

Given that initially, effects of a spider toxin, PT1, on P2X3 currents in rat sensory neurons were explored at virtually saturating agonist concentrations [19], we examined a modulatory action of PT1 and PT2 on recombinant P2X3 receptors under similar conditions. We first generated dose–response curves for mP2X3/hP2X3 receptors to determine agonist concentrations saturating CTP/ATP-gated currents in our heterologous system. CHO cells transfected with mP2X3 or hP2X3 were stimulated by CTP or ATP applied at different concentrations to generate dose–response curves (Suppl. Fig. 2). Based on these dependencies, mP2X3 and hP2X3 currents were stimulated in further experiments by a brief application of 100 μM CTP and 10 μM ATP, respectively.

An important feature of P2X3 receptors is the high-affinity desensitization. This phenomenon manifests itself through a marked decrease in a P2X3 current elicited by a short agonist pulse, if ambient agonist is present in the bath at subthreshold nanomolar concentrations [27,28]. Because this type of P2X3 desensitization turned out to be critically important for interpretation of PT1 and PT2 effects (see below), we studied this phenomenon in separate experiments. In a typical trial, a cell transfected with mP2X3 (hP2X3) was stimulated by 100 μM CTP (10 μM ATP) at least twice in control to obtain the averaged magnitude of a P2X3 current (Fig. 2A, B, upper panels). Although affected a resting current negligibly, the addition of subthreshold CTP (ATP) to the bath led to a marked decrease in cellular responsivity to 100 μM CTP (10 μM ATP) due to high-affinity desensitization. The cell was stimulated 2–3 times to determine the averaged value of the desensitized P2X3 current. Next, the ambient nucleotide was carefully rinsed, and 100 μM CTP (10 μM ATP) was applied again to reveal whether P2X3 current rundown took place (Fig. 2A, B, upper panels). Note that ambient nucleotide not only decreased responses to 100 μM CTP (10 μM ATP) but also slowed down their desensitization (Fig. 2A, B, bottom panels). As reported previously, the high-affinity desensitization of P2X3 is accompanied by slowing down the recovery of P2X3 currents from classical desensitization [28]. To prevent a possible influence of variable recovery of P2X3 from desensitization on current magnitude, we stimulated P2X3-positive cells by nucleotides as rarely as once per ~5 min and carefully rinsed them afterward. Such an assay required prolonged recordings so that rundown of P2X currents could occur. Therefore, a given cell was assayed only at one particular concentration of ambient CTP (ATP), and for further analysis, we took solely those cells that exhibited almost complete recovery of a P2X3 current after removal of an ambient agonist (Fig. 2A, B, upper panels).

Quantitatively, the high-affinity desensitization was characterized as the fractional inhibition $\boldsymbol{F}$ of a P2X3 current by an ambient agonist at a given concentration $\boldsymbol{A}$:

$$F = \frac{I_0 - I_A}{I_0} = \frac{A^n}{A_{1/2}^n + A^n} \quad (1)$$

where $I_o$ is the averaged P2X3 current in control, $I_A$ is the averaged P2X3 current desensitized by ambient CTP or ATP, $n$ is the Hill coefficient, $A_{1/2}$ is the half-inhibition concentration. Fig. 2C summarizes overall experimental data (symbols) that characterize the high-affinity desensitization of the mP2X3 current occurring in the presence of ambient CTP. As a function of nanomolar CTP, the fractional inhibition $F$ was fitted with Eq. (1) (solid line), giving $n = 2.2$, $A_{1/2} = 46.5$ nM. The similar analysis of hP2X3 currents (Fig. 2B) yielded the following values: $n = 1.9$, $A_{1/2} = 2.67$ nM ATP (Fig. 2D).

### 3.3. Effects of PT1 and PT2 on activity of P2X3 receptors

As found in earlier experiments with rat sensory neurons, P2X3 currents were markedly reduced in the presence of PT1 that also slowed down P2X3 recovery from desensitization [19]. These PT1 effects were dose-dependent with $IC_{50} = 12$ nM. We therefore expected PT1 to modulate P2X3 receptors from other mammalians, the mouse and human, and considered the possibility that another spider toxin, PT2, also could be effective.

Theoretically, these polypeptides could affect P2X3 currents by means of changing the number of available channels, altering affinity to the particular agonist and/or influencing a degree and/or kinetics of desensitization. For excluding a change in P2X current magnitude

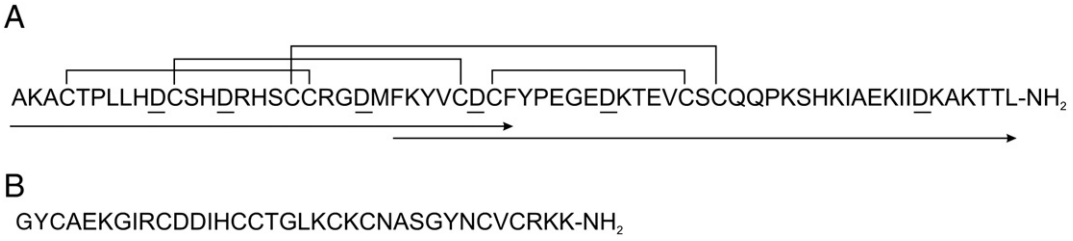


**Fig. 1.** PT1 and PT2 amino acid sequence. (A) Arrows below the PT2 sequence represent fragments determined by Edman degradation. Aspartic acid residues are underlined. C-terminal amidation is represented as $-NH_2$. The lines above indicate putative disulfide bonds. (B) PT1 sequence.

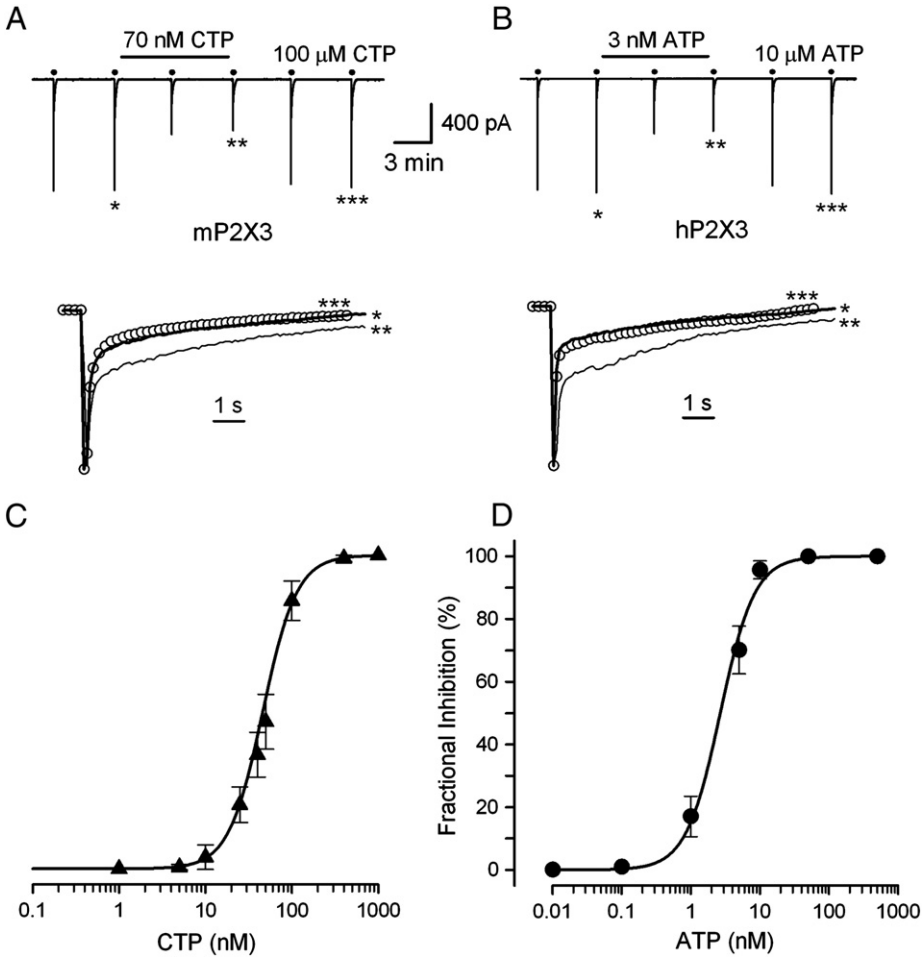


**Fig. 2.** High-affinity desensitization of P2X3 receptors. (A, B) Upper panels, the representative examples of sequential mP2X3 (hP2X3) currents stimulated by a 2-s pulse of 100 μM CTP (10 μM ATP) in control, in the presence of 70 nM CTP (3 nM ATP), and after rinse of the ambient nucleotide. The applications of CTP (ATP) are marked by the straight lines above the current traces. Cells were held at −30 mV, perfused with a solution containing 140 mM NaCl, and dialyzed with a solution containing 140 mM CsCl. Bottom panels, the particular CTP (ATP) responses from A (B) are superimposed in an enhanced time scale. The thick and thin lines and the circles correspond to the responses marked by *, ** and *** respectively. Each response was normalized to its peak value. (C, D) P2X3 current elicited by 100 μM CTP (10 μM ATP) versus ambient CTP (ATP) concentration. The data are presented as a mean ± s.d. ($n = 3$–5). The experimental dependencies (symbols) were fitted (solid lines) using Eq. (1) at $n = 2.2$, $A_{1/2} = 46.5$ nM in **C** and $n = 1.9$, $A_{1/2} = 2.67$ nM in D.

due to variable kinetics of recovery from desensitization, we stimulated P2X3-positive cells rarely enough and carefully rinsed them from an agonist. When CTP-gated currents through mP2X3 were elicited every 5 min, neither PT1 ($n = 7$) (Fig. 3A) nor PT2 ($n = 5$) (not shown) exerted statistically significant effects on cellular responses, which magnitude and kinetics varied with time slightly and to the same degree as control P2X3 currents (Fig. 3A, B, E). Meanwhile, both polypeptides markedly decreased magnitude of mP2X3 currents elicited by 100 μM CTP and slowed down their inactivation, provided that nanomolar CTP was present in the bath ($n = 37$) (Fig. 3C, D, E). This suggested that PT1 and PT2 affected CTP-gated currents largely by enhancing the high-affinity desensitization of mP2X3 receptors.

Indeed, as shown in Fig. 3D, the control CTP response (marked by *) inactivated more rapidly compared to the response (**) obtained with 50 nM CTP in the bath, while the additional deceleration of response inactivation (***) was exerted by 50 nM PT2. Importantly, this action of PT2 on kinetics of CTP-gated currents was reversible (Fig. 3C and D, left panel). To quantify effects of ambient CTP and PT2 on mP2X3 inactivation, the falling phase of a P2X3 current $I(t)$ was fitted at $t \geq t_p$ using the equation:

$$I(t)/I_p = \delta e^{-t/\tau_1} + (1-\delta)e^{-t/\tau_2} \quad (2)$$

where $I_p$ is the peak current at the moment $t_p$. The kinetic analysis of normalized cellular responses to 100 μM CTP in control and in the presence of 50 nM CTP or 50 nM CTP + 50 nM PT2 (Fig. 3D, right panel) yielded the following averaged parameters ($n = 4$), respectively: $\delta = 0.85 \pm 0.04$. $\tau_1 = 0.17 \pm 0.01$ s, $\tau_2 = 2.40 \pm 0.07$ s; $\delta = 0.68 \pm 0.03$, $\tau_1 = 0.19 \pm 0.02$ s, $\tau_2 = 3.32 \pm 0.11$; $\delta = 0.65 \pm 0.03$, $\tau_1 = 0.26 \pm 0.03$ s, $\tau_2 = 4.88 \pm 0.14$ s. Thus, the effect of ambient CTP on the kinetics of P2X3 current inactivation largely reduced to augmenting a contribution of the second exponential component, compared to control, and increasing its characteristic time $\tau_2$. PT2 markedly enhanced the effects of ambient CTP on mP2X3 current inactivation. Although we did not perform the similar kinetic analysis of effects of PT1 on mP2X3 current desensitized by 50 nM CTP, decelerated inactivation of those was well evident in all cases ($n = 7$), when both 50 nM CTP and 50 nM PT1 were present in the bath (not shown).

In addition, we generated an inhibitory curve for fractional inhibition of the mP2X3 current by ambient CTP in the presence of 50 nM PT1. It turned out that PT1 shifted the inhibitory curve of high-affinity desensitization to lower nucleotide concentrations (Fig. 3F). The fit of the experimental data with Eq. (1) showed that $IC_{50}$ for ambient CTP was decreased from 46.5 nM in control to 12.7 nM in the presence of 50 nM PT1.

The hP2X3 receptor was examined in a similar manner. As was the case with CTP-gated currents through mP2X3 receptors (Fig. 3A, E), 50 nM PT1 or 50 nM PT2 alone negligibly affected the magnitude of ATP-gated currents and kinetics of their inactivation, provided that hP2X3-positive cells were carefully rinsed from ATP (Fig. 4A, E). However,

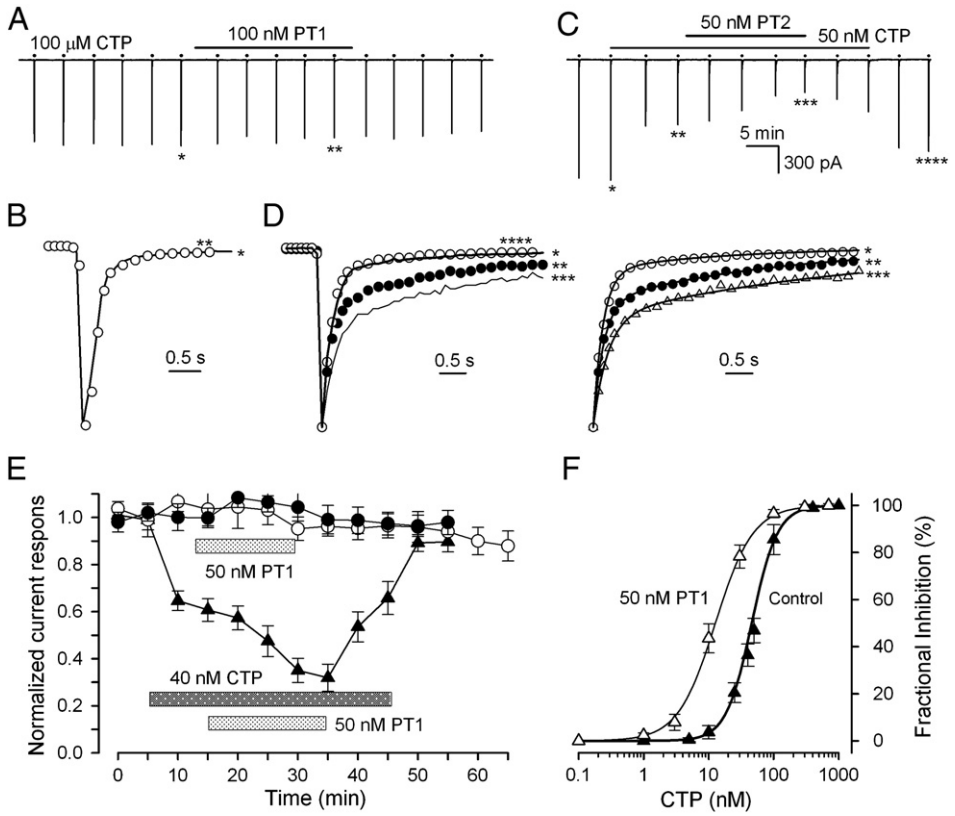


**Fig. 3.** Effects of PT1 and PT2 on the mP2X3 receptor. (A) Representative recording demonstrating an insignificant effect of PT1 on mP2X3 activity in the absence of ambient CTP. The P2X3 currents were elicited by a 2-s application of 100 μM CTP followed by continuous rinse with bath solution for ~5 min. The applications of CTP and 100 nM PT1 are marked by the dots and straight lines above the current traces. (B) Superimposition in an enhanced time scale of the particular CTP responses from A, each being normalized to its peak value. The solid line and circles correspond to the responses marked by * and **, respectively. (C) 50 nM PT2 enhanced the high-affinity desensitization of CTP-gated currents elicited by ambient CTP at 50 nM. (D) Left panel, the superimposition of the normalized CTP responses marked in C by * (thick line), ** (●), *** (thin line), and **** (o). Right panel, the falling phases of the CTP responses in control (o), in the presence of 50 nM CTP (●) or 50 nM CTP + 50 nM PT1 (Δ). These experimental curves were fitted with the Eq. (2) (solid lines) at the following parameters, correspondingly: $\delta = 0.87, 0.69, 0.61$; $\tau_1 = 0.18, 0.19, 0.27$ s; $\tau_2 = 2.42, 3.27, 4.95$ s. (E) Time evolution of mP2X3 currents exhibiting weak or negligible rundown in control (o) ($n = 6$), in the presence of 50 nM PT1 (●) ($n = 7$), and in the presence 40 nM CTP and 50 nM PT1 (▲) ($n = 5$) applied as indicated. The data are presented as a mean ± s.d. No statistically significant difference between time courses of CTP responses in control (o) and in the presence of 50 nM PT1 (●) was found ($p < 0.05$, Student-$t$-test). In the particular recording, all CTP responses were normalized to the half sum of the first two responses to 100 μM CTP. (F) mP2X3 current elicited by 100 μM CTP versus ambient CTP concentration in control (▲) and in the presence of 50 nM PT1 (Δ). The solid lines correspond to Eq. (1) at $n = 2.2, A_{1/2} = 46.5$ nM (thick line) and $n = 1.6, A_{1/2} = 12.7$ nM (thin line). In A–F, cells were held at −30 mV, perfused with a solution containing 140 mM NaCl, and dialyzed with a solution containing 140 mM CsCl.

when ambient ATP was present in the bath, both polypeptides decreased the magnitude of hP2X3 currents and slowed down their falling phases (Fig. 4C, D, E). The kinetic analysis of cellular responses to 10 μM ATP showed that under different conditions, the response inactivation was well described by Eq. (2) (Fig. 4D, right panel), giving the following parameters on average ($n = 3$): $\delta = 0.85 \pm 0.04$. $\tau_1 = 0.16 \pm 0.02$ s, $\tau_2 = 2.53 \pm 0.06$ s in control, $\delta = 0.72 \pm 0.04$. $\tau_1 = 0.18 \pm 0.02$ s, $\tau_2 = 3.48 \pm 0.09$ in the presence 2 nM ATP, and $\delta = 0.64 \pm 0.03$, $\tau_1 = 0.25 \pm 0.03$ s, $\tau_2 = 4.75 \pm 0.12$ s with 2 nM ATP + 50 nM PT1 in the bath. Qualitatively, PT2 exerted similar deceleration of hP2X3 current inactivation ($n = 5$) (not shown). The comparison of the inhibitory curves for ambient ATP generated in control and in the presence of PT2 revealed a decrease of $IC_{50}$ from 2.67 nM to 0.77 nM, respectively (Fig. 4F). Thus, the spider toxins could inhibit the hP2X3 receptor by enhancing its high-affinity desensitization, as was the case with mP2X3 receptors (Fig. 3).

### 3.4. Effects of PT1 and PT2 on activity of mP2X2/3 oligomeric receptors

Reportedly, certain P2X subunits form heteromeric ATP-gated channels. The list particularly includes the P2X2/P2X3 heteromer, which is involved in a variety of cellular functions, such as inflammatory and neuropathic pain, urinary bladder reflex, enteric neurotransmission and peristalsis, chemoreception, and taste transduction (reviewed in [29,30]). Given the inhibitory effects of PT1 and PT2 on desensitized P2X3 receptors (Fig. 3 and 4), we examined effects of these toxins on the mP2X2/mP2X3 heteromer.

The separate transfection of CHO cells with mP2X2 or with mP2X3 rendered them specifically responsive to external ATP. In contrast to mP2X3-positive cells (Fig. 3), activation of ATP-gated currents in mP2X2-positive cells was relatively slow, and they inactivated much less profoundly (Suppl. Fig. 3A). These findings are completely consistent with the observations of others [3,30]. When co-transfected with mP2X2 and mP2X3, CHO cells showed ATP-gated currents that were kinetically distinct from those mediated by homomeric P2X receptors (Suppl. Fig. 3A). Because ATP responses of the double-transfected cells could not be fitted using any linear combination of mP2X2 and mP2X3 currents (Suppl. Fig. 3B), we inferred that just heteromeric mP2X2/mP2X3 receptors were largely responsible for such ATP-gated currents.

In agreement with previous results [19], 100 nM PT1 negligibly affected ATP-gated currents through mP2X2 and mP2X2/3 receptors, and 100 nM PT2 also exhibited negligible effects (not shown). In light of results obtained with P2X3 currents (Fig. 3 and 4), we attempted to elucidate whether ambient ATP could promote any effects of PT1 or PT2 on mP2X2/3 receptors. It turned out that at subthreshold concentrations, ambient ATP affected negligibly ATP-gated currents per se. Moreover, neither PT1 (not shown) nor PT2 (Fig. 5A) exerted specific modulation of mP2X2/3 currents, judging by their magnitude and kinetics (Fig. 5B, C), in the presence of nanomolar ATP. Thus, our overall

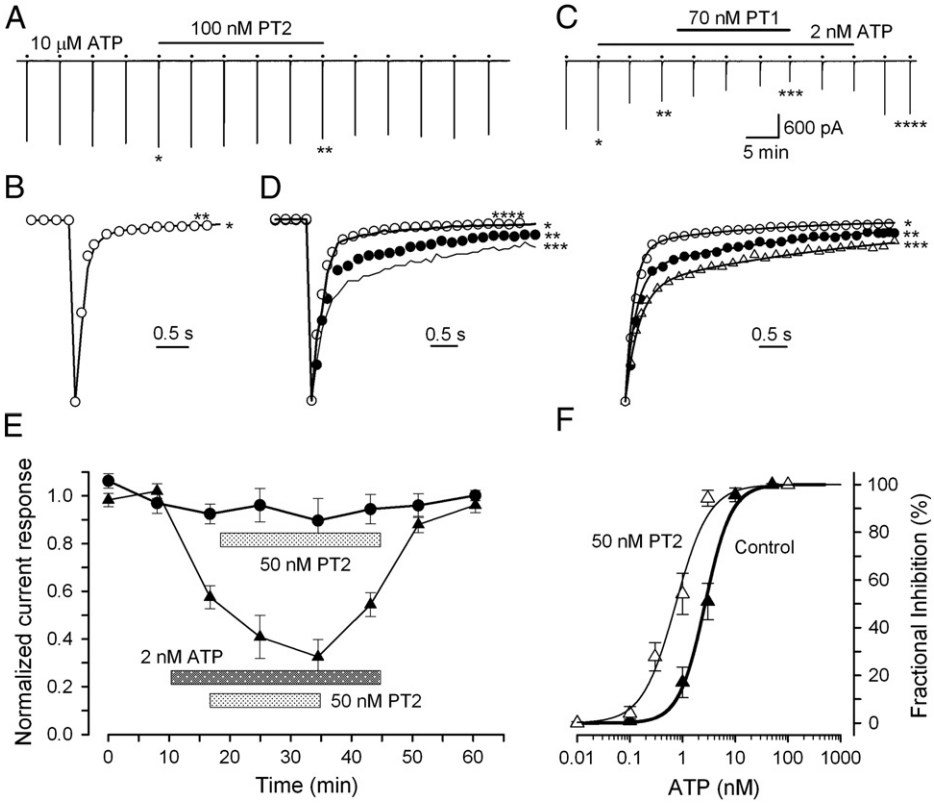


**Fig. 4.** Effects of PT1 and PT2 on the hP2X3 receptor. (A) PT2 affected negligibly hP2X3 currents elicited by a 2-s application of 10 μM ATP followed by continuous rinse with the bath solution for ~5 min. 10 μM ATP and 100 nM PT2 were applied as indicated. (B) Superimposition of the particular ATP responses from A. The solid line and circles correspond to the responses marked by * and **, respectively. Each response was normalized to its peak value. (C) 70 nM PT1 enhanced the high-affinity desensitization of ATP-gated currents in the presence of ambient ATP at 2 nM. (D) Left panel, the superimposition of the particular ATP responses from C normalized to the peak value. Right panel, the falling phases of the ATP responses in control (o) and in the presence of 2 nM ATP (●) or 2 nM ATP + 70 nM PT1 (Δ). The experimental curves were fitted with the Eq. (2) (solid lines) at the following parameters, correspondingly: $\delta = 0.86, 0.72, 0.63$; $\tau_1 = 0.16, 0.18, 0.25$ s; $\tau_2 = 2.53, 3.48, 4.76$ s. (E) Evolution of hP2X3 currents with time in control (●) ($n = 5$) and in the presence of 2 nM ATP and 50 nM PT2 (▲) ($n = 6$) applied as indicated. The data are presented as a mean ± s.d. In the particular recording, all ATP responses were normalized to the half sum of the first two responses to 10 μM ATP. (F) hP2X3 current elicited by 10 μM ATP versus ambient ATP concentration in control (▲) and in the presence of 50 nM PT2 (Δ). The solid lines correspond to Eq. (1) at $n = 1.7$, $A_{1/2} = 2.67$ nM (thick line) and $n = 1.4$, $A_{1/2} = 0.77$ nM (thin line). Recording conditions were as in Fig. 3.

data point out that the P2X3 receptor is a specific target for both PT1 and PT2 toxins.

## 4. Discussion

Ample evidence indicates that ATP is a nociceptive messenger and that purinergic signaling is associated with nociception and pain (for review see [31,32]. It was particularly shown that exogenous ATP introduced into the skin generates burning pain in humans; both ATP and α,β-methylene ATP, a P2X agonist, stimulated nociceptors in the rat skin [33,34]. Administration of ADP-β-S, a P2Y1, P2Y12 and P2Y13 agonist, inhibited spinal nociceptive transmission and nocifensive behavior [35], and infusion of the P2Y1 agonist MRS2365, P2Y12 antagonist MRS2395, and P2Y2/P2Y4 agonist UTP significantly alleviated mechanical allodynia in the neuropathic pain model [36].

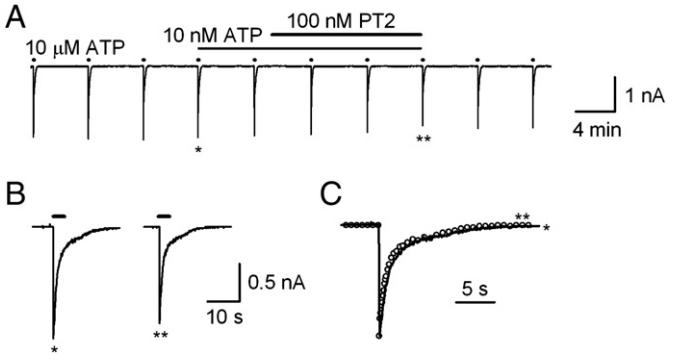


**Fig. 5.** PT2 does not modulate the heteromeric mP2X2/mP2X3 receptor. (A) Representative ($n = 16$) ATP responses of a CHO cell transfected with the mP2X2 and mP2X3 subunits. The ATP-gated currents were elicited by a 6-s application of 10 μM ATP marked by the straight lines above the recordings. (B) Particular ATP responses of the mP2X2/mP2X3-positive cell indicated by the asterisks in A are presented in an enhanced time scale. (C) Superimposition of the ATP responses shown in B, each being normalized to its magnitude. Recording conditions were as in Fig. 3.

Nociceptive neurons predominantly express P2X2 and P2X3 subunits [37,38]. Several experimental models corroborate the involvement of P2X2 and P2X3 receptors in the development of nerve injury-induced mechanical hypersensitivity. It was shown that nocifensive behavioral responses developed after injury could be reversed by P2X receptor antagonists, and inhibition of P2X2 and P2X3 led to a reduction in Aδ and C-fiber activity elicited by nerve injury [37,39]. Somewhat similar results were obtained in studies of animals deficient in P2X2 and P2X3 receptors [17,40]. Although P2X3 receptor antagonists do not affect acute pain sensitivity, they definitely have analgesic action in inflammatory and neuropathic pain models [39,41]. Thus, selective antagonists for P2X3 and/or P2X2/3 receptors may constitute a basis for novel analgesic drugs [31].

### 4.1. PT2 is a novel peptide modulator of mammalian P2X3 receptors

P2X3 receptors are targeted by a great number of low-molecular-weight substances with a varying degree of affinity and specificity [42]. Prior to this work, only two peptides have been reported to specifically modulate activity of mammalian P2X3 receptors, namely, purotoxin-1 (PT1) [19] and spinorphin [43]. The latter is known to inhibit enkephalin-degrading enzymes as well [44]. Purotoxin-2 (PT2)

described here is in fact a novel polypeptide from structural and functional points of view. Despite common origin, that is, the *Geolycosa* sp. venom, there is no significant similarity between PT2 and PT1, except for the PSM and ESM motifs and the ICK signature. Meanwhile, PT2 shows close similarity with certain LSTX toxins from *Lycosa singoriensis* identified by transcriptome analysis of the venom glands [45]. Lower but still considerable similarity takes place between PT2 and CSTX toxins from *Cupiennius salei* [46], including the CSTX-13 toxic enhancer [47]. It is interesting whether some LSTX and/or CSTX toxins are capable of modulating P2X3 receptors. If so, PT2 can be considered as the founder of a new purotoxin family.

### *4.2. PT1 and PT2 promote the high-affinity desensitization of P2X3 receptors*

Based on physiological activity of PT1 revealed with animal models and sensory neurons [19], we questioned whether PT1 and PT2 might modulate recombinant P2X3 receptors. We expressed heterologously murine and human P2X3 receptors in CHO cells. Note that unlike hP2X3, ATP-gated currents through mP2X3 were characterized by an inappropriately long refractory period, thus preventing a recording of a suitable number of reproducible cellular responses. For this reason, mP2X3 and hP2X3 were stimulated by CTP and ATP, respectively.

Two different modes have been reported for the PT1 action on P2X3 currents in rat DRG neurons [19]: when applied to nondesensitized receptors, PT1 potentiated P2X3 currents, while current inhibition took place, if the desensitized receptor was treated with PT1. Here we studied recombinant mP2X3 and hP2X3 receptors and found that neither PT1 nor PT2 (up to 100 nM) exerted statistically significant potentiation or inhibition of CTP or ATP-gated currents, provided that ambient CTP or ATP was carefully rinsed (Fig. 3A, B and 4A, B). Perhaps, somewhat different recording protocols and/or difference between species-related P2X3 receptors and/or cell-specific microenvironment underlay the mentioned inconsistency between the data present here and the results obtained with rat DRG neurons [19].

In our experiments, P2X-positive cells became evidently sensitive to the spider toxins, only if CTP/ATP was present in the bath at subtheshold nanomolar concentrations. With ambient nucleotides in the external solution, the addition of 50–70 nM PT1 or PT2 to the bath invariably resulted in a marked reduction of CTP/ATP-gated currents and deceleration of their inactivation (Fig. 3C, D and 4C, D). This indicated that ambient nucleotide was a necessary cofactor rendering P2X3 receptors sensitive to the spider toxins. Both PT1 and PT2 appeared to enhance the high-affinity desensitization of P2X3 receptors. It was particularly found that at the concentration of 50 nM, the polypeptides, PT1 for mP2X3 and PT2 for hP2X3, shifted inhibitory curves for the high-affinity desensitization of P2X3 receptors, eliciting a nearly 3-fold decrease in the $IC_{50}$ dose for an ambient nucleotide (Fig. 3F and 4F).

The elucidated mode of the inhibitory action of PT1 and PT2 on P2X3 activity is rather exceptional: they exert no effects on slow-desensitizing P2X2 and P2X2/3 subtypes of purinoreceptors (Fig. 5) but selectively affect the fast-desensitizing P2X3 subtype, most likely by recognizing solely a desensitized conformation of the receptor. To our knowledge, only $P^1$,$P^5$-di[inosine-5′] pentaphosphate, a noncompetitive antagonist of fast-desensitizing P2X1 and P2X3 purinoceptors, is capable of acting in a somewhat similar mode by binding the desensitized conformation [48]. However, the relatedness of its effects to the high-affinity desensitization remains non-investigated.

In conclusion, our data indicate that the larger fraction of P2X3 receptors gets the high-affinity desensitization, the more profound effects of the PT1 and PT2 toxins on P2X3 currents could be expected. Although ATP abundance in intercellular milieu is not known with confidence, the estimates available for certain tissues range a concentration of ambient ATP from hundreds pM to dozens nM [49,50]. This points out that in vivo, the high-affinity desensitization may control P2X3 receptor functions in response to a phasic ATP release, especially in inflammatory tissues. If so, administration of PT1 and PT2 should enhance the high-affinity desensitization of P2X3. This may account for the analgesic effect of the PT1 peptide documented in the animal model of inflammation [19].

## Acknowledgements

This work was supported by the Program "Molecular and Cell Biology" of the Russian Academy of Sciences (awards to EVG and SSK), the Federal Oriented Program "Scientific and Educational Personnel in Innovative Russia" (award to OAR), the Russian Foundation for Basic Research (grant nos. 11-04-00057 to SSK and 10-04-01105 to MFB), Russian Federal Program of the Ministry of Education and Science (contract no. 16.512.11.2195).

## Appendix A. Supplementary data

Supplementary data to this article can be found online at http://dx.doi.org/10.1016/j.bbamem.2012.07.016.

## References

[1] G. Burnstock, Introduction: P2 receptors, Curr. Top. Med. Chem. 4 (2004) 793–803.
[2] L. Erb, Z. Liao, C.I. Seye, G.A. Weisman, P2 receptors: intracellular signaling, Pflugers Arch. 452 (2006) 552–562.
[3] R.A. North, Molecular physiology of P2X receptors, Physiol. Rev. 82 (2002) 1013–1067.
[4] J.R. Gever, D.A. Cockayne, M.P. Dillon, G. Burnstock, A.P. Ford, Pharmacology of P2X channels, Pflugers Arch. 452 (2006) 513–537.
[5] R.A. North, A. Surprenant, Pharmacology of cloned P2X receptors, Annu. Rev. Pharmacol. Toxicol. 40 (2000) 563–580.
[6] X. Bo, A. Alavi, Z. Xiang, I. Oglesby, A. Ford, G. Burnstock, Localization of ATP-gated P2X2 and P2X3 receptor immunoreactive nerves in rat taste buds, Neuroreport 10 (1999) 1107–1111.
[7] G. Burnstock, Endothelium-derived vasoconstriction by purines and pyrimidines, Circ. Res. 103 (2008) 1056–1057.
[8] C.C. Chen, A.N. Akopian, L. Sivilotti, D. Colquhoun, G. Burnstock, J.N. Wood, A P2X purinoceptor expressed by a subset of sensory neurons, Nature 377 (1995) 428–431.
[9] Y.H. Jin, T.W. Bailey, B.Y. Li, J.H. Schild, M.C. Andresen, Purinergic and vanilloid receptor activation releases glutamate from separate cranial afferent terminals in nucleus tractus solitarius, J. Neurosci. 24 (2004) 4709–4717.
[10] C. Lewis, S. Neidhart, C. Holy, R.A. North, G. Buell, A. Surprenant, Coexpression of P2X2 and P2X3 receptor subunits can account for ATP-gated currents in sensory neurons, Nature 377 (1995) 432–435.
[11] L. Vulchanova, M.S. Riedl, S.J. Shuster, L.S. Stone, K.M. Hargreaves, G. Buell, et al., P2X3 is expressed by DRG neurons that terminate in inner lamina II, Eur. J. Neurosci. 10 (11) (1998) 3470–3478.
[12] E.C. Wang, J.M. Lee, W.G. Ruiz, E.M. Balestreire, M. von Bodungen, S. Barrick, et al., ATP and purinergic receptor-dependent membrane traffic in bladder umbrella cells, J. Clin. Invest. 115 (9) (2005) 2412–2422.
[13] D.A. Cockayne, S.G. Hamilton, Q.M. Zhu, P.M. Dunn, Y. Zhong, S. Novakovic, A.B. Malmberg, G. Cain, A. Berson, L. Kassotakis, L. Hedley, W.G. Lachnit, G. Burnstock, S.B. McMahon, A.P. Ford, Urinary bladder hyporeflexia and reduced pain-related behaviour in P2X3-deficient mice, Nature 407 (2000) 1011–1015.
[14] X. Bian, J. Ren, M. DeVries, B. Schnegelsberg, D.A. Cockayne, A.P. Ford, J.J. Galligan, Peristalsis is impaired in the small intestine of mice lacking the P2X3 subunit, J. Physiol. 551 (2003) 309–322.
[15] T.E. Finger, V. Danilova, J. Barrows, D.L. Bartel, A.J. Vigers, L. Stone, G. Hellekant, S.C. Kinnamon, ATP signaling is crucial for communication from taste buds to gustatory nerves, Science 310 (2005) 1495–1499.
[16] J. Ren, X. Bian, M. DeVries, B. Schnegelsberg, D.A. Cockayne, A.P. Ford, J.J. Galligan, P2X2 subunits contribute to fast synaptic excitation in myenteric neurons of the mouse small intestine, J. Physiol. 552 (2003) 809–821.
[17] V. Souslova, P. Cesare, Y. Ding, A.N. Akopian, L. Stanfa, R. Suzuki, K. Carpenter, A. Dickenson, S. Boyce, R. Hill, D. Nebenuis-Oosthuizen, A.J. Smith, E.J. Kidd, J.N. Wood, Warm-coding deficits and aberrant inflammatory pain in mice lacking P2X3 receptors, Nature 407 (2000) 1015–1017.
[18] G. Burnstock, Physiology and pathophysiology of purinergic neurotransmission, Physiol. Rev. 87 (2007) 659–797.
[19] E.V. Grishin, G.A. Savchenko, A.A. Vassilevski, Y.V. Korolkova, Y.A. Boychuk, V.Y. Viatchenko-Karpinski, K.D. Nadezhdin, A.S. Arseniev, K.A. Pluzhnikov, V.B. Kulyk, N.V. Voitenko, O.O. Krishtal, Novel peptide from spider venom inhibits P2X3 receptors and inflammatory pain, Ann. Neurol. 67 (2010) 680–683.
[20] A.A. Vassilevski, S.A. Kozlov, T.A. Egorov, E.V. Grishin, Purification and characterization of biologically active peptides from spider venoms, Methods Mol. Biol. 615 (2010) 87–100.
[21] M.E. Gasparian, V.G. Ostapchenko, A.A. Schulga, D.A. Dolgikh, M.P. Kirpichnikov, Expression, purification, and characterization of human enteropeptidase catalytic subunit in Escherichia coli, Protein Expr. Purif. 31 (2003) 133–139.
[22] S.S. Kolesnikov, R.F. Margolskee, Extracellular $K^+$ activates a $K^+$- and $H^+$-permeable conductance in frog taste cells, J. Physiol. 507 (1998) 415–432.

[23] K. Pluzhnikov, A. Vassilevski, Y. Korolkova, A. Fisyunov, O. Iegorova, O. Krishtal, E. Grishin, omega-Lsp-IA, a novel modulator of P-type Ca2 + channels, Toxicon 50 (2007) 993–1004.
[24] S. Kozlov, E. Grishin, Classification of spider neurotoxins using structural motifs by primary structure features. Single residue distribution analysis and pattern analysis techniques, Toxicon 46 (2005) 672–686.
[25] S. Mouhat, B. Jouirou, A. Mosbah, M. De Waard, J.M. Sabatier, Diversity of folds in animal toxins acting on ion channels, Biochem. J. 378 (2004) 717–726.
[26] A.A. Vassilevski, S.A. Kozlov, E.V. Grishin, Molecular diversity of spider venom, Biochemistry (Mosc) 74 (2009) 1505–1534.
[27] E. Sokolova, A. Skorinkin, E. Fabbretti, L. Masten, A. Nistri, R. Giniatullin, Agonist-dependence of recovery from desensitization of P2X(3) receptors provides a novel and sensitive approach for their rapid up or downregulation, Br. J. Pharmacol. 141 (2004) 1048–1058.
[28] E.B. Pratt, T.S. Brink, P. Bergson, M.M. Voigt, S.P. Cook, Use-dependent inhibition of P2X3 receptors by nanomolar agonist, J. Neurosci. 25 (2005) 7359–7365.
[29] L.E. Browne, L.H. Jiang, R.A. North, New structure enlivens interest in P2X receptors, Trends Pharmacol. Sci. 31 (2010) 229–237.
[30] T.M. Egan, D.S. Samways, Z. Li, Biophysics of P2X receptors, Pflugers Arch. 452 (2006) 501–512.
[31] G. Burnstock, Purinergic receptors and pain, Curr. Pharm. Des. 15 (2009) 1717–1735.
[32] J. Scholz, C.J. Woolf, The neuropathic pain triad: neurons, immune cells and glia, Nat. Neurosci. 10 (2007) 1361–1368.
[33] S.G. Hamilton, S.B. McMahon, ATP as a peripheral mediator of pain, J. Auton. Nerv. Syst. 81 (2000) 187–194.
[34] S.G. Hamilton, S.B. McMahon, G.R. Lewin, Selective activation of nociceptors by P2X receptor agonists in normal and inflamed rat skin, J. Physiol. 534 (2001) 437–445.
[35] Z. Gerevich, S.J. Borvendeg, W. Schroder, H. Franke, K. Wirkner, W. Norenberg, S. Fürst, C. Gillen, P. Illes, Inhibition of N-type voltage-activated calcium channels in rat dorsal root ganglion neurons by P2Y receptors is a possible mechanism of ADP-induced analgesia, J. Neurosci. 24 (2004) 797–807.
[36] R.D. Ando, B. Mehesz, K. Gyires, P. Illes, B. Sperlagh, A comparative analysis of the activity of ligands acting at P2X and P2Y receptor subtypes in models of neuropathic, acute and inflammatory pain, Br. J. Pharmacol. 159 (2010) 1106–1117.
[37] Y. Chen, G.W. Li, C. Wang, Y. Gu, L.Y. Huang, Mechanisms underlying enhanced P2X receptor-mediated responses in the neuropathic pain state, Pain 119 (2005) 38–48.
[38] K. Kobayashi, T. Fukuoka, H. Yamanaka, Y. Dai, K. Obata, A. Tokunaga, K. Noguchi, Differential expression patterns of mRNAs for P2X receptor subunits in neurochemically characterized dorsal root ganglion neurons in the rat, J. Comp. Neurol. 481 (2005) 377–390.
[39] C.J. Sharp, A.J. Reeve, S.D. Collins, J.C. Martindale, S.G. Summerfield, B.S. Sargent, S.T. Bate, I.P. Chessell, Investigation into the role of P2X(3)/P2X(2/3) receptors in neuropathic pain following chronic constriction injury in the rat: an electrophysiological study, Br. J. Pharmacol. 148 (2006) 845–852.
[40] D.A. Cockayne, P.M. Dunn, Y. Zhong, W. Rong, S.G. Hamilton, G.E. Knight, H.Z. Ruan, B. Ma, P. Yip, P. Nunn, S.B. McMahon, G. Burnstock, A.P. Ford, P2X2 knockout mice and P2X2/P2X3 double knockout mice reveal a role for the P2X2 receptor subunit in mediating multiple sensory effects of ATP, J. Physiol. 567 (2005) 621–639.
[41] M.F. Jarvis, E.C. Burgard, S. McGaraughty, P. Honore, K. Lynch, T.J. Brennan, A. Subieta, T. Van Biesen, J. Cartmell, B. Bianchi, W. Niforatos, K. Kage, H. Yu, J. Mikusa, C.T. Wismer, C.Z. Zhu, K. Chu, C.H. Lee, A.O. Stewart, J. Polakowski, B.F. Cox, E. Kowaluk, M. Williams, J. Sullivan, C. Faltynek, A-317491, a novel potent and selective non-nucleotide antagonist of P2X3 and P2X2/3 receptors, reduces chronic inflammatory and neuropathic pain in the rat, Proc. Natl. Acad. Sci. U. S. A. 99 (2002) 17179–17184.
[42] Y.A. Andreev, A.A. Vassilevski, S.A. Kozlov, Molecules to selectively target receptors for treatment of pain and neurogenic inflammation, Recent Pat. Inflamm. Allergy Drug Discov. 6 (2012) 35–45.
[43] K.Y. Jung, H.D. Moon, G.E. Lee, H.H. Lim, C.S. Park, Y.C. Kim, Structure-activity relationship studies of spinorphin as a potent and selective human P2X(3) receptor antagonist, J. Med. Chem. 50 (2007) 4543–4547.
[44] K. Nishimura, T. Hazato, Isolation and identification of an endogenous inhibitor of enkephalin-degrading enzymes from bovine spinal cord, Biochem. Biophys. Res. Commun. 194 (1993) 713–719.
[45] Y. Zhang, J. Chen, X. Tang, F. Wang, L. Jiang, X. Xiong, M. Wang, M. Rong, Z. Liu, S. Liang, Transcriptome analysis of the venom glands of the Chinese wolf spider Lycosa singoriensis, Zoology (Jena) 113 (2010) 10–18.
[46] L. Kuhn-Nentwig, J. Schaller, W. Nentwig, Biochemistry, toxicology and ecology of the venom of the spider Cupiennius salei (Ctenidae), Toxicon 43 (2004) 543–553.
[47] B. Wullschleger, L. Kuhn-Nentwig, J. Tromp, U. Kampfer, J. Schaller, S. Schurch, W. Nentwig, CSTX-13, a highly synergistically acting two-chain neurotoxic enhancer in the venom of the spider Cupiennius salei (Ctenidae), Proc. Natl. Acad. Sci. U. S. A. 101 (2004) 11251–11256.
[48] K.K. Ford, M. Matchett, J.E. Krause, W. Yu, The P2X3 antagonist P1, P5-di[inosine-5′] pentaphosphate binds to the desensitized state of the receptor in rat dorsal root ganglion neurons, J. Pharmacol. Exp. Ther. 315 (2005) 405–413.
[49] E.R. Lazarowski, D.A. Shea, R.C. Boucher, T.K. Harden, Release of cellular UDP-glucose as a potential extracellular signaling molecule, Mol. Pharmacol. 63 (2003) 1190–1197.
[50] L. Seminario-Vidal, E.R. Lazarowski, S.F. Okada, Assessment of extracellular ATP concentrations, Methods Mol. Biol. 574 (2009) 25–36.